Chemical Engineering Journal 163 (2010) 317–323

Contents lists available at ScienceDirect

Chemical Engineering Journal

journal homepage: www.elsevier.com/locate/cej

Nitrate removal from water by nano-alumina: Characterization and sorption studies

Amit Bhatnagar[a,b,*], Eva Kumar[b], Mika Sillanpää[c]

[a] Institute of Environmental Technology and Energy Economics, Technische Universität Hamburg-Harburg (TUHH), 21073 Hamburg-Harburg, Germany
[b] LSRE – Laboratory of Separation and Reaction Engineering, Departamento de Engenharia Química, Faculdade de Engenharia da Universidade do Porto (FEUP), Rua Dr. Roberto Frias, 4200-465 Porto, Portugal
[c] Laboratory of Applied Environmental Chemistry (LAEC), Department of Environmental Sciences, University of Eastern Finland, Patteristonkatu 1, FI-50100 Mikkeli, Finland

ARTICLE INFO

Article history:
Received 31 May 2010
Received in revised form 1 August 2010
Accepted 3 August 2010

Keywords:
Nitrate removal
Nano-alumina
Sorption isotherms
Kinetic modeling
pH
Competing anions

ABSTRACT

The present study was conducted to evaluate the feasibility of nano-alumina for nitrate removal from aqueous solutions. The nature and morphology of sorbent was characterized by XRD, FTIR, BET and SEM analysis. Batch adsorption studies were performed as a function of contact time, initial nitrate concentration, temperature, pH and influence of other interfering anions. Nitrate sorption kinetics was well fitted by pseudo-second-order kinetic model. The maximum sorption capacity of nano-alumina for nitrate removal was found to be ca. 4.0 mg g^{-1} at 25 ± 2 °C. Maximum nitrate removal occurred at equilibrium pH ca. 4.4. The nitrate sorption has been well explained using Langmuir isotherm model. Results from this study demonstrated the potential utility of nano-alumina for nitrate removal from water.

1. Introduction

The presence of elevated concentrations of nitrate (NO_3^-) in potable water has become a serious concern worldwide over the past few decades. Nitrate is a water soluble ion that does not readily bind to the soil causing it to be highly susceptible to run-off migration [1]. Point and non-point sources of nitrate contamination can include agricultural and urban runoff, disposal of untreated sanitary and industrial wastes in unsafe manner, leakage in septic systems, landfill leachate, animal manure, NO*x* air stripping waste from air pollution control devices. Nitrate, due to its high water solubility, is possibly the most widespread groundwater contaminant in the world, imposing a serious threat to drinking water supplies and causing ecological disturbances [2,3]. Increasing nitrate concentrations in drinking water causes two adverse health effects: induction of "blue-baby syndrome" (methemoglobinemia), especially in infants, and the potential formation of carcinogenic nitrosamines [4,5].

Keeping the view of serious health problems associated with excess nitrate concentrations in drinking water, various environmental regulatory agencies including the U.S. Environmental Protection Agency (U.S. EPA) have set a maximum contaminant level (MCL) of 10 mg L^{-1} of nitrate-N in drinking water. Nitrate contaminated water must be treated properly to meet applicable regulations.

The commonly used treatment methods for nitrate removal include chemical denitrification using zero-valent iron (Fe^0) [6–8], zero-valent magnesium (Mg^0) [9], ionic exchange [10], reverse osmosis [11], electrodialysis [12], catalytic denitrification [13] and biological denitrification [14]. However, current available technologies for nitrate removal are found to be expensive, inefficient and generate additional by-products. Generally, reverse osmosis, ion exchange and electrodialysis processes are considered the best available technologies (BAT) to treat nitrate-contaminated water [15–17]. Nevertheless, these traditional technologies do not solve the problem related to the excess of nitrate in the environment; in turn, they produce nitrate concentrated waste streams that pose a disposal problem due to the high saline content [14,17,18]. BATs are relatively expensive [16] and moreover, cause process complexity to be used in in situ application for direct decontamination of groundwater [19].

Zero-valent iron (ZVI) has been extensively studied for its ability to reduce different contaminants including nitrate in groundwater [6–8,20–22]. However, this technology has some limitations as discussed by various researchers in different articles. For example, Cheng et al. [6] reported that the main disadvantages of nitrate reduction using ZVI are ammonium production and the pH control requirement (by initial pH reduction or using a buffer). When

* Corresponding author at: LSRE – Laboratory of Separation and Reaction Engineering, Departamento de Engenharia Química, Faculdade de Engenharia da Universidade do Porto (FEUP), Rua Dr. Roberto Frias, 4200-465 Porto, Portugal.
E-mail addresses: dr.amit10@gmail.com, amit_b10@yahoo.co.in (A. Bhatnagar).

1385-8947/$ – see front matter © 2010 Elsevier B.V. All rights reserved.
doi:10.1016/j.cej.2010.08.008

applying ZVI in an in situ remediation technique for nitrate removal, these disadvantages are even more critical [21]. Furthermore, biological denitrification processes are difficult to apply to inorganic wastewater treatment because additional organic substrates of electron donors are required [23].

Comparatively, adsorption seems to be a more attractive method for the removal of nitrate in terms of cost, simplicity of design and operation. Different adsorbents have been tested for the removal of nitrate from water [24–32]. Conventionally, nitrate removal by different adsorbents has been employed using micron-sized particles, however, in recent years, nanotechnology has emerged as one of the attractive technologies for water treatment. The benefits of using nano-materials may derive from their self-assembly, large surface area and enhanced reactivity [33] and can be potentially utilized for water remediation [34].

In the present study, adsorption feasibility of nano-alumina has been assessed for nitrate removal from aqueous solution. The characterization of nano-alumina in the form of scanning electron micrographs (SEM), X-ray diffraction (XRD), Fourier transform infra-red (FTIR) and Brunauer Emmett Teller (BET) has been conducted and its performance was further assessed for nitrate removal from water. Adsorption studies were conducted under various experimental conditions, such as pH, contact time, initial nitrate concentrations, temperature, and the presence of competing anions. The data from the experiments were fitted with different models to identify the adsorption mechanism. The results have been thoroughly discussed which would help in the better understanding of nitrate sorption mechanism by nano-alumina.

2. Material and methods

2.1. Materials

Nano-alumina (Al_2O_3 nanopowder) was purchased from Sigma–Aldrich. Nitrate stock solution was prepared by dissolving sodium nitrate (Sigma–Aldrich) in deionized (DI) water. Standards and nitrate spiked samples at a required concentration range were prepared by appropriate dilution of the stock solution with DI water. All reagents used were of analytical reagent grade.

2.2. Characterization of the adsorbent

The morphology of the sorbent was determined by scanning electron microscopy (SEM) using Quanta 200 (FEI, Netherlands) field-emission gun (FEG) scanning electron microscope. The X-ray diffraction (XRD) pattern of the nano-alumina was obtained using a Bruker AXS D8 Advance X-ray diffractometer. FTIR spectra of the sorbent was collected using Nicolet 8700 FTIR spectrometer (Thermo Instruments, USA). Nitrogen adsorption/desorption isotherms were obtained using a BEL Japan Inc. Belsorp-Max surface area analyzer at 77 K.

2.3. Nitrate analysis

The concentration of nitrate in the solutions was determined by ion chromatography (Dionex, ICS-90, Ion Chromatography system, USA). The mobile phase consisted of a mixture of 7.0 mM sodium carbonate (Na_2CO_3) and 2.0 mM sodium bicarbonate ($NaHCO_3$) delivered at the flow rate of 1.0 mL min^{-1}. AS40 autosampler (Dionex, USA) was assembled with a 10-μL injection loop. A separation column, IonPac® AS9-HC, 4.0 mm × 250 mm (Dionex, USA), a guard column, IonPac® AG9-HC, 4.0 mm × 50 mm (Dionex, USA), and membrane suppressor, AMMS III 4-mm were used. The data acquisition was performed using Chromeleon 6.5 (Dionex, USA).

2.4. Nitrate adsorption studies

Adsorption of nitrate onto nano-alumina was studied by batch experiments. A stock nitrate solution (1000 mg L^{-1}) was used in adsorption experiments. The required concentration of the nitrate solution was prepared by serial dilution of stock solution. A fixed amount of the adsorbent was added to nitrate solution taken in 50 mL capped tubes, which were placed in a thermostat cum shaking assembly. The solutions were stirred continuously at constant temperature to achieve equilibrium. After equilibrium, the solid was separated by centrifugation (5000 rpm) and filtration through IC Millex-LG filter (Millipore). The filtrates were kept in refrigerator at 2 °C for next day analysis. The concentration of the nitrate in the solution was analyzed by ion chromatography. Reproducibility of the measurements was determined in triplicates and the average values are reported. Relative standard deviations were found to be within ±3.0%. The amount of nitrate adsorbed (q_e in mg g^{-1}) was calculated as follows:

$$q_e = \frac{(C_0 - C_e) \cdot V}{m} \quad (1)$$

where C_0 and C_e are the initial and equilibrium concentrations of nitrate in solution (mg L^{-1}), V is the volume of solution (L) and m is mass of the adsorbent (g).

2.4.1. pH studies

In order to investigate the effect of pH on nitrate adsorption, the pH of the nitrate solutions (20 mg L^{-1}) were adjusted from 3 to 12. The initial pH of the solution was adjusted by using 0.1 M HCl or 0.1 M NaOH and nano-alumina (0.025 g) was added to 25 mL solution. The mixture was shaken using a temperature-controlled water bath shaker. After adsorption, the final pH of all solutions was measured and the value providing the maximum nitrate removal was determined.

2.4.2. Kinetic studies

The rate of adsorption of nitrate was studied at different time intervals (1 min–24 h). In kinetic studies, 25 mL nitrate solution (10 and 20 mg L^{-1}) with an initial solution pH of 3.1 were agitated with nano-alumina (0.025 g) using a temperature-controlled water bath shaker. After a fixed time interval, the adsorbent was separated as described in section 2.4 and the filtrate was analyzed to determine the equilibrium concentration of nitrate. Experiments were repeated for different periods until reaching the adsorption equilibrium.

2.4.3. Equilibrium adsorption studies

The adsorption of nitrate on nano-alumina was conducted at two temperatures (25 and 10 ± 2 °C) by batch experiments. Twenty five millilitres of nitrate solution of varying initial concentrations (1–100 mg L^{-1}) with an initial solution pH of 3.1 in 50 mL capped tubes were shaken with 0.025 g of adsorbent after adjusting the pH to the desired value, for a specified period of contact time in a temperature-controlled shaking assembly. After equilibrium, samples were filtered and the filtrate was then analyzed for residual nitrate concentration by ion chromatography.

2.4.4. Competing anions studies

The effects of competing anions (chloride, fluoride, carbonate, sulphate and phosphate) on nitrate adsorption were investigated by performing nitrate adsorption under a fixed nitrate concentration (20 mg L^{-1}), and initial competing anion concentrations of 20–100 mg L^{-1} with sorbent dosage of 1 g L^{-1}.

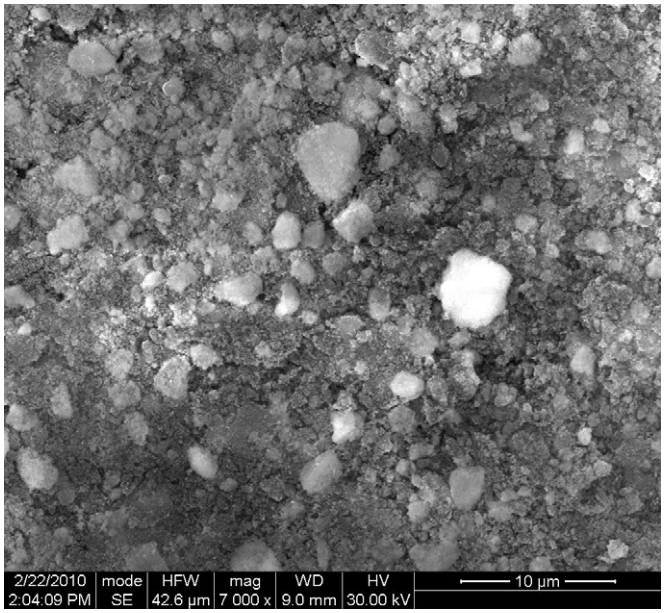

Fig. 1. SEM image of nano-alumina.

3. Results and discussion

3.1. Characterization of Al_2O_3 nanopowder

The SEM analysis of nano-alumina (Fig. 1) revealed that the sorbent does not possess any well defined porous structure (only few pores on the surface). The BET surface area and total pore volume of nano-alumina were found to be 151.7 $m^2\,g^{-1}$ and 1.09 $cm^3\,g^{-1}$, respectively. The phase analysis of nano-alumina was observed by XRD (Fig. 2) and it confirmed the presence of γ-alumina phase in the sorbent. The FTIR spectra of nano-alumina is shown in Fig. 3. The characteristic region for nano-Al_2O_3 powders lies in the wave number range from 400 to 1000 cm^{-1} [35]. The characteristic infrared absorption peak of nano-alumina was observed at 760 cm^{-1}. Further, two bands at 802 and 582 cm^{-1} also appear in the spectra, which are the characteristics of Al–O vibration in Al_2O_3 [36]. An absorption band at ca. 1620 cm^{-1} was also observed which is in accordance with the reported literature that alumina presents an absorption band at ca. 1620 cm^{-1} [37].

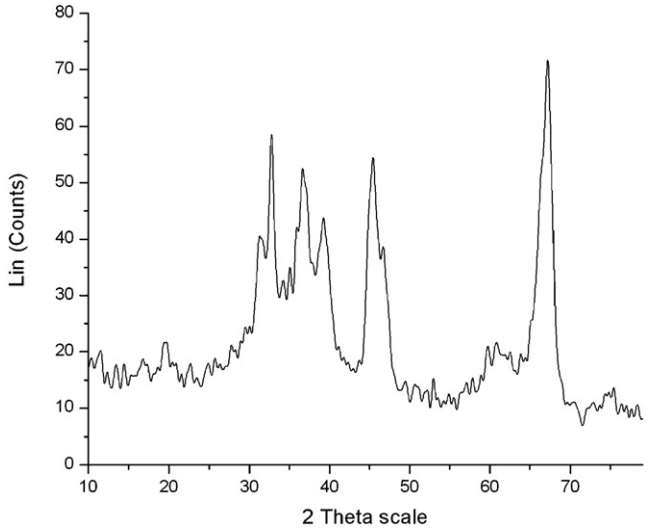

Fig. 2. XRD pattern of nano-alumina.

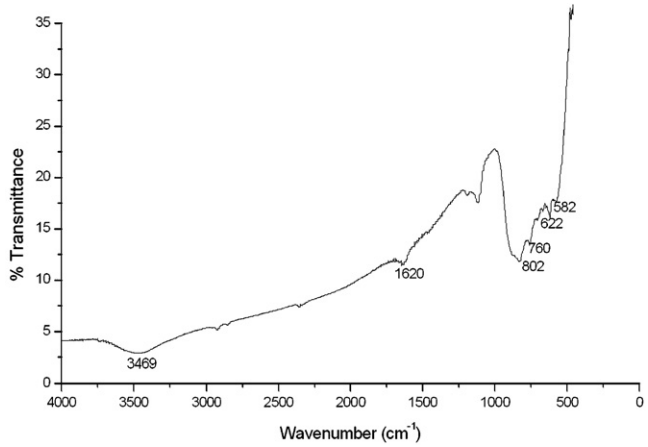

Fig. 3. FTIR spectra of nano-alumina.

3.2. Effect of pH

The pH is an important parameter influencing the sorption process at the water-adsorbent interfaces. To determine the optimum pH for the maximum removal of nitrate, the equilibrium adsorption of nitrate (with initial nitrate concentration of 20 mg L^{-1}) was investigated over a pH range of 3–12. It can be seen (Fig. 4) that the adsorption of nitrate on nano-alumina is strongly pH dependent. The adsorption of nitrate increased with increasing pH, reaching a maximum at equilibrium pH ca. 4.4 (initial pH = 3.1), and then decreased with further increase in pH. This may be due to the competition for the active sites by OH^- ions and the electrostatic repulsion of anionic nitrate by the negatively charged nano-alumina surface at higher pH. The decrease in nitrate adsorption is particularly sharp above pH 5.4, as the surface charge becomes more negative. Different pH_{pzc} values ranging from 5 to 9 are reported for aluminium based oxides/hydroxide in the literature [38,39]. Hence, nitrate ions would have to overcome electrostatic forces as there would be a higher density of negative charge very close to the surface, hence greater electrostatic repulsion.

3.3. Effect of contact time and initial nitrate concentration

The adsorption of nitrate on nano-alumina was investigated as a function of contact time (1 min–24 h) at two different initial nitrate concentrations (10 and 20 mg L^{-1}) with an initial solution pH of 3.1. It was noticed that nitrate removal increased with time (Fig. 5). The

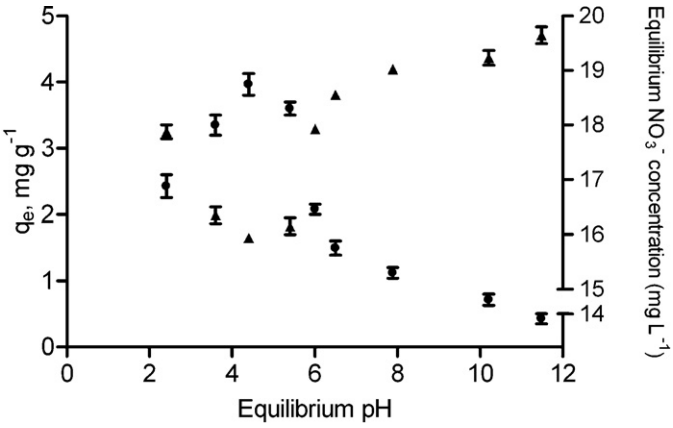

Fig. 4. Effect of pH on nitrate sorption on nano-alumina (temperature = 25 °C, contact time = 24 h, sorbent dose = 1 g L^{-1}) [●: q_e, mg g^{-1}; ▲: equilibrium NO_3^- concentration, mg L^{-1}].

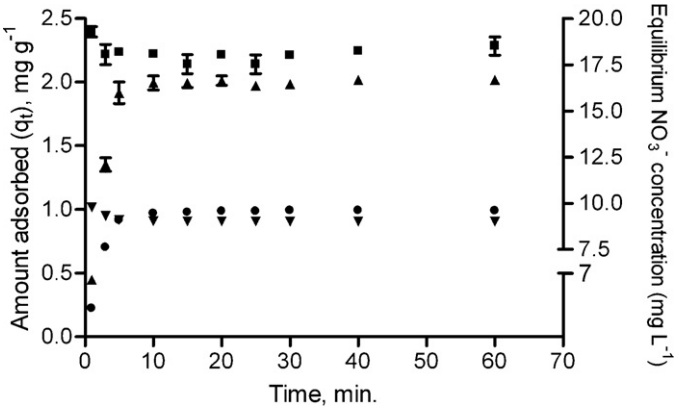

Fig. 5. Effect of contact time and initial nitrate concentration on sorption of nitrate on nano-alumina (temperature = 25 °C, sorbent dose = 1 g L^{-1}, equilibrium pH = ~4.4) [●: amount adsorbed at time (q_t, mg g^{-1}) ($C_{initial}$ = 10.0 mg L^{-1}); ▲: amount adsorbed at time (q_t, mg g^{-1}) ($C_{initial}$ = 20.0 mg L^{-1}); ▼: equilibrium NO_3^- concentration (mg L^{-1}) ($C_{initial}$ = 10.0 mg L^{-1}); ■: equilibrium NO_3^- concentration (mg L^{-1}) ($C_{initial}$ = 20.0 mg L^{-1})].

trends of the plots in Fig. 5 exhibit that nitrate uptake was rapid in the beginning followed by a slower removal that gradually reached a plateau. Maximum removal of nitrate was achieved within the first 15 min of contact time and equilibrium was attained in 60 min. There was no significant change in nitrate uptake by nano-alumina in the following 24 h.

The effect of initial nitrate concentration on equilibrium adsorption was also investigated at two different initial nitrate concentrations (10 and 20 mg L^{-1}). Nitrate uptake by nano-alumina increased when the initial nitrate concentration increased from 10 to 20 mg L^{-1} (Fig. 5). This behaviour can be explained due to the increase in the driving force of the concentration gradient, as an increase in the initial nitrate concentration. Such phenomenon is common in a batch reactor with either constant adsorbent dose or varying initial adsorbate concentration or vice versa [40].

3.4. Kinetic modeling

The kinetics of nitrate sorption on nano-alumina was analyzed using pseudo-first-order [41] and pseudo-second-order [42] kinetic models. The best-fit model was selected based on the match between experimental ($q_{e(exp)}$) and theoretical ($q_{e(cal)}$) uptake values and linear correlation coefficient (R^2) values at two studied concentrations. The values obtained by pseudo-second-order model (Fig. 6) were found to be in good agreement with experimental data and can be used to favorably explain the nitrate sorption on nano-alumina. The rate equations and the related values are given in Table 1.

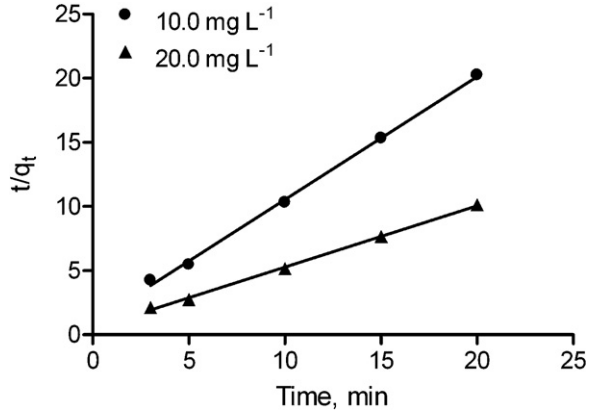

Fig. 6. Pseudo-second-order kinetic plots of sorption of nitrate on nano-alumina.

Table 1
Pseudo-second-order and Weber and Morris model parameters, and calculated $q_{e(cal)}$ and experimental $q_{e(exp)}$ values for different initial nitrate concentrations.

C_0 (mg L^{-1})	$q_{e(exp)}$ (mg g^{-1})	k_s (g mg^{-1} min^{-1})	$q_{e(cal)}$ (mg g^{-1})	R^2
Pseudo-second-order model: $\frac{t}{q_t} = \frac{1}{k_s q_e^2} + \frac{1}{q_e} t$				
10	1.03	0.93	1.04	0.9985
20	1.98	0.47	2.09	0.9981
C_0 (mg L^{-1})	k_{ip1} (mg g^{-1} $min^{-0.5}$)	R^2	k_{ip2} (mg g^{-1} $min^{-0.5}$)	R^2
Weber and Morris model: $q_t = k_{ip} t^{1/2} + C$				
10	0.57	0.9986	0.02	0.9922
20	1.13	0.9879	0.03	0.9990

q_e: Amount of nitrate adsorbed on nano-alumina (mg g^{-1}) at equilibrium, q_t: amount of nitrate adsorbed on nano-alumina (mg g^{-1}) at time t (min), k_s: rate constant for the pseudo-second-order kinetics, k_{ip}: intra-particle diffusion rate constant, C: intercept related to the thickness of the boundary layer.

The intra-particle diffusion approach [43] can be used to predict if intra-particle diffusion is the rate-limiting step. The data exhibit multi-linear plots, revealing that the process is governed by two or more steps (Fig. 7). The first linear portion (phase I) at both concentrations, can be attributed to the immediate utilization of the most readily available sorbing sites on the sorbent surface. Phase II may be attributed to very slow diffusion of the sorbate from the surface site into the inner pores. Thus initial portion of nitrate sorption by nano-alumina may be governed by the initial intra-particle transport of nitrate controlled by surface diffusion process and the later part controlled by pore diffusion. The values of k_{ip1} and k_{ip2} (diffusion rate constants for phases I and II, respectively) obtained from the slope of linear plots are listed in Table 1.

3.5. Adsorption isotherms

In order to evaluate the adsorption capacity of nano-alumina for nitrate, the equilibrium adsorption of nitrate was studied as a function of nitrate concentration and the adsorption isotherms are shown in Fig. 8. An adsorption capacity of ca. 4.0 mg g^{-1} was observed for nitrate on nano-alumina at 25 ± 2 °C. The initial sharp rise in the isotherm indicates the availability of readily accessible sites for adsorption. However, site saturation occurs as the nitrate concentration increases and a plateau is reached indicating that no more sites remain available for adsorption. The interaction between nitrate and metal oxide can be modeled as a two-step

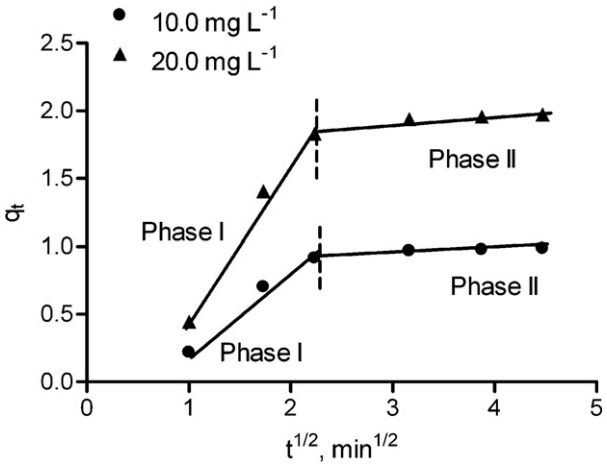

Fig. 7. Weber and Morris intra-particle diffusion plots of sorption of nitrate on nano-alumina.

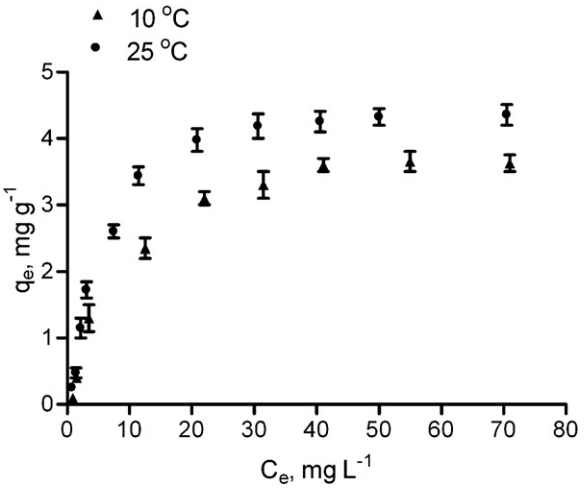

Fig. 8. Sorption isotherms of nitrate on nano-alumina (contact time = 24 h, sorbent dose = 1 g L^{-1}, equilibrium pH = ~4.4).

ligand exchange reactions as shown below [24]:

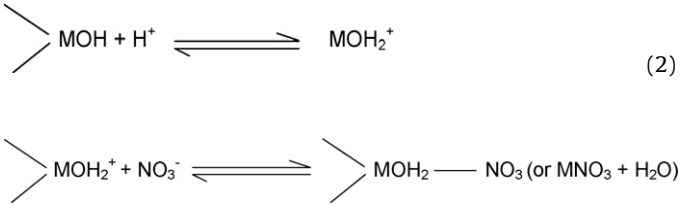

(2)

(3)

where M presents metal ions (Al).

In order to investigate the effect of temperature on nitrate removal by nano-alumina, adsorption experiments were also performed at 10 °C. A comparison of adsorption isotherms at 10 and 25 °C indicates that nitrate sorption by nano-alumina is slightly affected (Fig. 8). The sorption data was further analyzed using Langmuir model, which can be expressed as follows:

$$\frac{1}{q_e} = \frac{1}{q_m} + \frac{1}{q_m b C_e} \tag{4}$$

where q_e is amount sorbed at equilibrium concentration C_e, q_m is the Langmuir constant representing maximum monolayer sorption capacity, b is the Langmuir constant related to energy of sorption. The experimental data was fitted well with Langmuir model. The plots of $1/q_e$ as a function of $1/C_e$ for the sorption of nitrate on nano-alumina (not shown here) were found linear with good correlation coefficients (>0.99) indicating the applicability of Langmuir model in the present study. The values of monolayer capacity (q_m) and Langmuir constant (b) are given in Table 2. The values of q_m calculated by the Langmuir isotherm were all close to experimental values at given temperatures. These facts suggest that nitrate is sorbed in the form of monolayer coverage on the surface of the sorbent.

The influence of adsorption isotherm shape has been discussed [44] to examine whether adsorption is favorable in terms of 'R_L', a dimensionless constant referred to as separation factor or equilibrium parameter. 'R_L' is calculated using the equation below:

$$R_L = \frac{1}{1 + bC_0} \tag{5}$$

The R_L values obtained are compiled in Table 2. The R_L values lie between 0 and 1 confirming that the adsorption isotherm is favorable.

Table 2
Langmuir constants for the adsorption of nitrate on nano-alumina at 10 and 25 °C.

Temperature (°C)	Langmuir constants			
	q_m (mg g^{-1})	b (L mol^{-1})	R_L	R^2
10	4.57	4.37×10^3	0.67	0.9995
25	5.48	6.12×10^3	0.59	0.9985

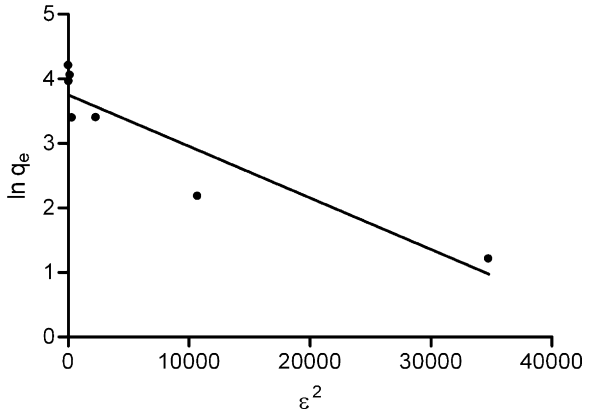

Fig. 9. Dubinin–Redushkevich (D–R) isotherm of nitrate sorption on nano-alumina.

The nature of adsorption (physical or chemical) was also analyzed by Dubinin–Radushkevich (D–R) isotherm. The linear form of (D–R) isotherm equation can be expressed as [45–47].

$$\ln q_e = \ln q_m - \beta\varepsilon^2 \tag{6}$$

where q_e is the amount of nitrate adsorbed per unit mass of adsorbent, q_m is the theoretical adsorption capacity, β is the constant of the sorption energy, which is related to the average energy of sorption per mole of the adsorbate as it is transferred to the surface of the solid from infinite distance in the solution [46], and ε is Polanyi potential, which is described as:

$$\varepsilon = RT \ln\left(1 + \frac{1}{C_e}\right) \tag{7}$$

where T is the temperature (K) and R is the gas constant. The value of mean sorption energy, E, can be calculated from D–R parameter β as follows:

$$E = \frac{1}{\sqrt{-2\beta}} \tag{8}$$

The value of E is very useful in predicting the type of adsorption and if the value is from 1 to 8 kJ mol^{-1}, then the adsorption is physical in nature and if it is from 8 to 16 kJ mol^{-1}, then the adsorption is chemical in nature [45–47]. Fig. 9 shows the plot of ln q_e versus ε^2. The value of E was found to be 4.07 kJ mol^{-1} suggesting the physical nature of the adsorption process in the present study.

3.6. Thermodynamic parameters

The nature and thermodynamic feasibility of the sorption process were determined by evaluating the thermodynamic constants, standard free energy (ΔG^o), standard enthalpy (ΔH^o) and standard entropy (ΔS^o) using Eqs. (9)–(11):

$$\Delta G^o = -RT \ln(K) \tag{9}$$

$$\ln\left(\frac{K_2}{K_1}\right) = -\frac{\Delta H^o}{R}\left(\frac{1}{T_2} - \frac{1}{T_1}\right) \tag{10}$$

$$\Delta G^o = \Delta H^o - T\Delta S^o \tag{11}$$

where R is the universal gas constant (8.314 J mol^{-1} K^{-1}), T is the temperature in Kelvin and K is the equilibrium constant. The values

Table 3
Thermodynamic parameters for the adsorption of nitrate on nano-alumina at different temperatures.

Temperature (°C)	ΔG^o (kJ mol^{-1})	ΔS^o (J mol^{-1} K^{-1})	ΔH^o (kJ mol^{-1})
10	−29.17	158.71	15.74
25	−31.55	158.71	

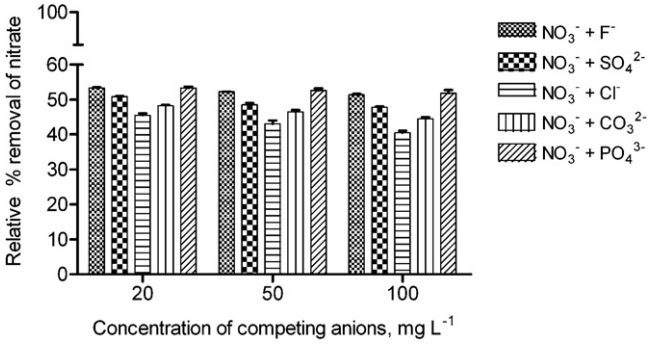

Fig. 10. Effect of different concentrations of competing anions on nitrate sorption on nano-alumina (temperature = 25 °C, contact time = 24 h, sorbent dose = 1 g L^{-1}.

of the above stated parameters are summarized in Table 3. The adsorption process is spontaneous in nature, as indicated by the negative value of ΔG^o. The positive value of ΔH^o suggested that the interaction of nitrate and nano-alumina is endothermic in nature. In literature [48], when the value of ΔH^o is lower than 40 kJ mol^{-1} the type of adsorption can be accepted as a physical process. Since ΔH^o value obtained in this study is lower than 40 kJ mol^{-1}, it would be claimed that the physical adsorption occurs during adsorption. Affinity of the adsorbent for nitrate is represented by the positive value of ΔS^o.

3.7. Effect of competing anions on nitrate adsorption by nano-Al_2O_3

The impact of various anions including chloride (Cl^-), fluoride (F^-), sulphate (SO_4^{2-}), carbonate (CO_3^{2-}) and phosphate (PO_4^{3-}) on nitrate removal by nano-alumina was investigated at 20 mg L^{-1} of initial nitrate concentration. The concentration of competing anions was varied from 20 to 100 mg L^{-1} (Fig. 10). It was observed that nitrate adsorption was mainly influenced by the presence of chloride, sulphate and carbonate ions. Anions present in the nitrate solutions are likely to limit the nitrate removal efficiency. In the presence of chloride, percent removal of nitrate was ~40–45%, while in case of other anions (sulphate and carbonate) percent removal of nitrate was ~45–50%. This indicates that the outer-spherically sorbing anions especially chloride and sulphate can significantly interfere the sorption of nitrate at elevated concentrations where the sorption competition can be occurred for the limited amount of sorption sites on nano-alumina. On the other hand, phosphate and fluoride (inner-spherically sorbing anions) show little interference on nitrate sorption.

4. Conclusions

The results from the present study exhibit the potential of nano-alumina for nitrate removal from aqueous solutions. The sorption of nitrate on nano-alumina was found to be pH dependent with maximum nitrate removal occurring at pH 4.4. Kinetic analyses indicate that the sorption process followed pseudo-second-order kinetics. The sorption capacity of nano-alumina for nitrate was found to be ca. 4.0 mg g^{-1} at 25 °C. Nitrate sorption was affected by the presence of chloride, sulphate and carbonate anions. The results of the present study suggest that nano-alumina can be used for the removal of excess nitrates from water.

Acknowledgments

A part of this research work was partially conducted at Institute of Environmental Technology and Energy Economics (IUE), TUHH, Hamburg-Harburg, Germany and authors express their sincere thanks to IUE staff for providing necessary help. One of the authors (AB) is also thankful to FCT (Fundação para a Ciência e a Technologia), Lisbon, Portugal, for the award of post-doctoral grant (FCT-DFRH-SFRH/BPD/62889/2009).

References

[1] A. Nuhoglu, T. Pekdemir, E. Yildiz, B. Keskinler, G. Akay, Drinking water denitrification by a membrane bio-reactor, Water Res. 36 (2002) 1155–1166.
[2] A. Liu, M. Ming, R.O. Ankumah, Nitrate contamination in private wells in rural Alabama, United States, Sci. Total Environ. 346 (2005) 112–120.
[3] A. Kapoor, T. Viraraghavan, Nitrate removal from drinking water. A review, J. Environ. Eng., ASCE 123 (1997) 371–380.
[4] D. Majumdar, N. Gupta, Nitrate pollution of groundwater and associated human health disorders, Indian J. Environ. Health 42 (2000) 28–39.
[5] C.H. Tate, K.F. Arnold, in: F.W. Pontius (Ed.), Health and Aesthetic Aspects of Water Quality. Water Quality and Treatment, McGraw-Hill Inc., New York, 1990, pp. 63–156.
[6] I.F. Cheng, R. Muftikian, Q. Fernando, N. Korte, Reduction of nitrate to ammonia by zero valent iron, Chemosphere 35 (1997) 2689–2695.
[7] Y.H. Huang, T.C. Zhang, Effects of low pH on nitrate reduction by iron powder, Water Res. 38 (2004) 2631–2642.
[8] Y.M. Chen, C.W. Li, S.S. Chen, Fluidized zero valent iron bed reactor for nitrate removal, Chemosphere 59 (2005) 753–759.
[9] M. Kumar, S. Chakraborty, Chemical denitrification of water by zero valent magnesium powder, J. Hazard. Mater. B135 (2006) 112–121.
[10] M. Dore, Ph Simon, A. Deguin, J. Victot, Removal of nitrate in drinking water by ion exchange-impact on the chemical quality of treated water, Water Res. 20 (1986) 221–232.
[11] J.J. Schoeman, A. Steyn, Nitrate removal with reverse osmosis in a rural area in South Africa, Desalination 155 (2003) 15–26.
[12] F. Hell, J. Lahnsteiner, H. Frischherz, G. Baumgartner, Experience with full-scale electrodialysis for nitrate and hardness removal, Desalination 117 (1998) 173–180.
[13] A. Pintar, J. Batista, J. Levec, Catalytic denitrification: direct and indirect removal of nitrates from potable water, Catal. Today 66 (2001) 503–510.
[14] M.I.M. Soares, Biological denitrification of groundwater, Water Air Soil Pollut. 123 (2000) 183–193.
[15] L.W. Canter, Nitrates in Groundwater, CRC Press, Boca Raton, 1997.
[16] K.S. Haugen, M.J. Semmens, P.J. Novak, A novel *in-situ* technology for the treatment of nitrate contaminated groundwater, Water Res. 36 (2002) 3497–3506.
[17] C.D. Rocca, V. Belgiorno, S. Meriç, Overview of *in-situ* applicable nitrate removal processes, Desalination 204 (2007) 46–62.
[18] B.A. Till, L.J. Weathers, P.J.J. Alvarez, Fe(0)-supported autotrophic denitrification, Environ. Sci. Technol. 32 (1998) 634–639.
[19] W.J. Hunter, Use of vegetable oil in a pilot-scale denitrifying barrier, J. Contam. Hydrol. 53 (2001) 119–131.
[20] C.-H. Liao, S.-F. Kang, Y.-W. Hsu, Zero-valent iron reduction of nitrate in the presence of ultraviolet light, organic matter and hydrogen peroxide, Water Res. 37 (2003) 4109–4118.
[21] S. Lee, K. Lee, S. Rhee, J. Park, Development of a new zero-valent iron zeolite material to reduce nitrate without ammonium release, J. Environ. Eng. ASCE 133 (2007) 6–12.
[22] H. Park, Y.-M. Park, S.-K. Oh, K.-M. You, S.-H. Lee, Enhanced reduction of nitrate by supported nanoscale zero-valent iron prepared in ethanol–water solution, Environ. Technol. 30 (2009) 261–267.
[23] F. Thalasso, A. Vallecillo, P. Garcia-Encina, F. Fdz-Polanco, The use of methane as a sole carbon source for wastewater denitrification, Water Res. 31 (1997) 55–66.
[24] Y. Cengeloglu, A. Tor, M. Ersoz, G. Arslan, Removal of nitrate from aqueous solution by using red mud, Sep. Purif. Technol. 51 (2006) 374–378.
[25] A. Bhatnagar, M. Ji, Y.-H. Choi, W. Jung, S.-H. Lee, S.-J. Kim, G. Lee, H. Suk, H.-S. Kim, B. Min, S.-H. Kim, B.-H. Jeon, J.W. Kang, Removal of nitrate from water by adsorption onto zinc chloride treated activated carbon, Sep. Sci. Technol. 43 (2008) 886–907.
[26] K. Mizuta, T. Matsumoto, Y. Hatate, K. Nishihara, T. Nakanishi, Removal of nitrate-nitrogen from drinking water using bamboo powder charcoal, Bioresour. Technol. 95 (2004) 255–257.
[27] N. Öztürk, T.E. Bektaş, Nitrate removal from aqueous solution by adsorption onto various materials, J. Hazard. Mater. B112 (2004) 155–162.
[28] Y. Xi, M. Mallavarapu, R. Naidu, Preparation, characterization of surfactants modified clay minerals and nitrate adsorption, Appl. Clay Sci. 48 (2010) 92–96.

[29] K. Hosni, E. Srasra, Nitrate adsorption from aqueous solution by M^{II}–Al–CO_3 layered double hydroxide, Inorg. Mater. 44 (2008) 742–749.
[30] M.M. Socías-Viciana, M.D. Ureña-Amate, E. González-Pradas, M.J. García-Cortés, C. López-Teruel, Nitrate removal by calcined hydrotalcite-type compounds, Clay Clay Miner. 56 (2008) 2–9.
[31] M. Islam, R. Patel, Nitrate sorption by thermally activated Mg/Al chloride hydrotalcite-like compound, J. Hazard. Mater. 169 (2009) 524–531.
[32] M. Islam, P.C. Mishra, R. Patel, Physicochemical characterization of hydroxyapatite and its application towards removal of nitrate from water, J. Environ. Manage. 91 (2010) 1883–1891.
[33] K. Hristovski, A. Baumgardner, P. Westerhoff, Selecting metal oxide nanomaterials for arsenic removal in fixed bed columns: from nanopowders to aggregated nanoparticle media, J. Hazard. Mater. 147 (2007) 265–274.
[34] X. Zhao, J. Wang, F. Wu, T. Wang, Y. Cai, Y. Shi, G. Jiang, Removal of fluoride from aqueous media by Fe_3O_4@$Al(OH)_3$ magnetic nanoparticles, J. Hazard. Mater. 173 (2010) 102–109.
[35] C.H. Shek, J.K.L. Lai, T.S. Gu, G.M. Lin, Transformation evolution and infrared absorption spectra of amorphous and crystalline nano-Al_2O_3 powders, Nanostruct. Mater. 8 (1997) 605–610.
[36] C.L. Lu, J.G. Lv, L. Xu, X.F. Guo, W.H. Hou, Y. Hu, H. Huang, Crystalline nanotubes of γ-AlOOH and γ-Al_2O_3: hydrothermal synthesis, formation mechanism and catalytic performance, Nanotechnology 20 (2009) 1–9.
[37] T. Tsuchida, Preparation and reactivity of acicular α-Al_2O_3 from synthetic diaspore, β-Al_2O_3·H_2O, Solid State Ionics 63 (1993) 464–470.
[38] J. Hlavay, K. Polyak, Determination of surface properties of iron hydroxide coated alumina adsorbent prepared for removal of arsenic from drinking water, J. Colloid Interface Sci. 284 (2005) 71–77.
[39] S.M. Maliyekkal, S. Shukla, L. Philip, I.M. Nambi, Enhanced fluoride removal from drinking water by magnesia-amended activated alumina granules, Chem. Eng. J. 140 (2008) 183–192.
[40] K.H. Chu, Removal of copper from aqueous solution by chitosan in prawn shell: adsorption equilibrium and kinetics, J. Hazard. Mater. B90 (2002) 77–95.
[41] S. Lagergren, About the theory of so-called adsorption of soluble substances, K. Svenska. Vetenskapsakad. Handl. 24 (1898) 1–39.
[42] Y.S. Ho, G. McKay, Pseudo-second-order model for sorption processes, Process Biochem. 34 (1999) 451–465.
[43] W.J. Weber Jr., J.C. Morris, Kinetics of adsorption on carbon from solution, J. Sanit. Eng. Div. 89 (1963) 31–59.
[44] T.W. Weber, R.K. Chakravorti, Pore and solid diffusion models for fixed bed adsorbents, J. Am. Inst. Chem. Eng. 20 (1974) 228–238.
[45] H. Zheng, D. Liu, Y. Zheng, S. Liang, Z. Liu, Sorption isotherm and kinetic modeling of aniline on Cr-bentonite, J. Hazard. Mater. 167 (2009) 141–147.
[46] M.M. Dubinin, E.D. Zaverina, L.V. Radushkevich, Sorption and structure of active carbons. I. Adsorption of organic vapors, Zh. Fiz. Khim. 21 (1947) 1351–1362.
[47] K. Saltalı, A. Sarı, M. Aydın, Removal of ammonium ion from aqueous solution by natural Turkish (Yıldızeli) zeolite for environmental quality, J. Hazard. Mater. 141 (2007) 258–263.
[48] Z. Bekçi, Y. Seki, M.K. Yurdakoç, A study of equilibrium and FTIR, SEM/EDS analysis of trimethoprim adsorption onto K10, J. Mol. Struct. 827 (2007) 67–74.